https://doi.org/10.64504/big.dv3i1.322

Adaptive Morphology Control of Photo-Driven Lattice Flexible Sensor Arrays: Intelligent Contact Optimization for Wearable Physiological Signal Monitoring

1st Reginald Makoa
The National University of Lesotho
Roma, Lesotho
reginald.makoa2@outlook.com

2nd Fangtian Ying *
European Academy of Engineering
Gothenburg, Sweden
yingft@gmail.com

Received on September 6th, revised on October 21st, accepted on November 12th, published on January 6th.

***Abstract*—Flexible wearable sensors have demonstrated tremendous potential in personalized health monitoring, but their signal acquisition accuracy critically depends on the dynamically changing contact quality between the sensor and skin. Existing flexible sensors predominantly employ passive adaptation strategies, which struggle to actively optimize contact states in complex physiological scenarios such as motion and sweating, leading to signal quality degradation or even monitoring failure. To address this challenge, this study proposes an active morphology control method for flexible sensor arrays based on photo-driven lattice metamaterials. We constructed a truncated octahedral lattice structure with both high flexibility and photothermal responsiveness using poly (N-isopropylacrylamide)-single-walled carbon nanotube (PNIPAM-SWNT) hydrogel, and integrated conductive polymer (PEDOT:PSS) as sensing electrodes. Through precise scanning of 780nm femtosecond laser, local controllable deformation of the sensor array can be achieved. Experimental results show that the lattice structure design reduces the relative density of the sensor array to 18.5%, with photo-driven deformation amplitude reaching 35.2% and response speed of 12.8 μm/s. Through various morphology control modes such as local protrusion, bending, and torsion, the contact impedance between sensor and skin was effectively reduced by 62.3%, and the signal-to-noise ratio (SNR) of electrocardiogram (ECG) signals improved by 18.7 dB during motion states. This study innovatively extends photo-driven soft material technology from the microrobotics field to wearable electronics, providing a new paradigm for developing next-generation intelligent wearable devices with active adaptation capabilities, embodying deep interdisciplinary integration of design, materials, electronics, and biomedicine.**

Keywords*—Photo-driven sensor, Lattice metamaterial, Flexible electronics, Adaptive morphology control, Wearable health monitoring

1. Introduction

With the intensification of global population aging trends and the universal enhancement of health awareness, wearable health monitoring technology is transitioning from professional medical fields to consumer markets, becoming a key component of digital health and preventive medicine [1, 2]. Flexible wearable sensors can conformally attach to human skin surfaces, enabling non-invasive, continuous monitoring of key physiological parameters such as electrocardiogram (ECG), electromyogram (EMG), body temperature, and blood pressure, providing unprecedented technical means for chronic disease management, exercise status assessment, and early disease warning [3, 4]. The core challenge of these devices lies in how to consistently maintain high-quality signal acquisition capabilities in complex dynamic environments caused by daily human activities (such as walking, joint bending, sweating). The contact interface between sensor and skin is the "last mile" determining signal quality, and minor changes in contact state, such as relative sliding, pressure fluctuations, or sweat accumulation, can lead to dramatic increases in contact impedance, introducing severe motion artifacts and baseline drift, or even causing signal interruption [5].

According to established skin–sensor interface impedance models, contact impedance is jointly governed by effective contact area, local pressure distribution, and skin hydration conditions, all of which are highly dynamic during motion and perspiration. Therefore, ensuring stable and effective contact between sensors and skin in dynamic application scenarios has become a core bottleneck constraining the development of wearable technology.

To address this challenge, current research mainly focuses on passive flexibility design of materials and structures. Researchers have developed intrinsically soft conductive materials, such as conductive polymers, metal nanowire networks, and carbon-based composites, combined with special structural engineering like wavy, serpentine, or island-bridge layouts, endowing sensors with excellent stretchability

*Fangtian Ying, European Academy of Engineering, Gothenburg, Sweden, yingft@gmail.com

and bendability to passively adapt to skin deformation [6, 7]. For example, Wang et al. developed a microcrack-based strain sensor capable of maintaining conductivity over large deformation ranges [8]. Ha et al. utilized buckled structures on pre-stretched substrates to achieve highly stretchable electrode arrays [9].

However, the effectiveness of these passive adaptation strategies highly depends on initial fitting conditions and inherent mechanical properties of materials. Once significant body movement or skin surface environmental changes (such as sweating) occur, this preset flexibility is often insufficient to compensate for complex stresses generated at the interface, leading to contact instability and signal distortion.

More fundamentally, passive structures lack the ability to dynamically regulate contact pressure and contact area in response to real-time physiological changes, resulting in unavoidable performance degradation under prolonged or repeated motion conditions. Therefore, there is an urgent need for "intelligent" sensing technology capable of actively responding to environmental changes and dynamically adjusting its morphology to optimize contact states.

Active morphology control technology provides new insights for solving the above problems. By integrating shape memory alloys, electroactive polymers (EAP), or magnetically responsive materials, researchers have attempted to enable flexible devices with autonomous shape-changing capabilities [10, 11]. For example, dielectric elastomer actuators (DEAs) based on electro-deformation can achieve rapid, large-range deformation, but typically require high driving voltages (kV level), posing safety hazards [12]. Magnetic driving systems can achieve wireless control but have limited spatial resolution and require external bulky magnetic field generation devices, limiting their application in wearable fields [13].

In recent years, photo-responsive soft materials, particularly hydrogels based on photothermal effects, have received widespread attention in the soft robotics field due to their wireless driving, high spatial resolution, and material system diversity [14, 15]. Through precise control of laser irradiation position, intensity, and scanning path, complex, multi-modal motion control of hydrogel soft robots can be achieved, such as peristalsis, rotation, and jumping [16].

Compared with electrical and magnetic actuation schemes, photo-driven approaches offer a unique combination of wireless operation, micrometer-scale spatial resolution, and localized energy delivery, making them particularly attractive for fine-grained morphology regulation in soft systems. This high-precision spatiotemporal controllability provides an ideal technical foundation for local morphology control of flexible sensors.

However, migrating photo-driven technology from micrometer-scale soft robots to centimeter-scale wearable sensors faces new challenges. On one hand, the deformation speed and amplitude of traditional solid hydrogels are limited by their slow internal heat transfer and water molecule diffusion processes, making it difficult to meet the rapid response requirements of wearable applications [17]. On the other hand, most existing research focuses on driving performance itself, lacking work that combines morphology control with sensing functions and systematically studies its impact on signal quality. Additionally, most photo-driven systems remain at the laboratory demonstration stage, and their stability and reliability in real physiological environments need verification.

Meanwhile, lattice metamaterials have shown tremendous potential in aerospace and soft robotics fields due to their excellent mechanical properties such as lightweight, high strength, and designability [18, 19]. Through rational design of lattice microscopic topological structures, abnormal mechanical properties can be achieved macroscopically, such as negative Poisson's ratio and ultra-high damping.

Introducing lattice architectures into photo-responsive hydrogels provides a promising strategy to overcome intrinsic material limitations by reducing relative density, enhancing effective surface area, and enabling deformation modes dominated by structural rotation rather than bulk compression. Introducing lattice structures into photo-responsive hydrogels is expected to significantly improve photothermal conversion efficiency and driving response speed by reducing material relative density and increasing specific surface area, thereby overcoming performance bottlenecks of traditional hydrogel actuators [20].

This study aims to fill the gap in the application of photo-driven technology for active morphology control in wearable sensing fields. To the best of our knowledge, this work represents the first systematic integration of photo-driven lattice metamaterials with flexible wearable sensor arrays for active contact optimization. We propose and implement a flexible sensor array based on photo-driven lattice metamaterials, achieving active morphology control of sensors through laser scanning to optimize their contact quality with skin. Specifically, we designed and manufactured a truncated octahedral lattice structure based on PNIPAM-SWNT hydrogel and integrated a conductive polymer sensing layer. We systematically studied the influence of lattice structure parameters on photo-driven deformation performance and explored various laser scanning strategies to achieve multi-modal deformations such as local protrusion, bending, and torsion.

By attaching sensors to human skin, we quantitatively evaluated the optimization effect of active morphology control on contact impedance and verified its quality improvement effect in collecting various physiological signals such as ECG, EMG, and body temperature.

This study focuses on non-invasive, transcutaneous physiological signal monitoring, with particular emphasis on mitigating motion-induced artifacts and contact instability in dynamic scenarios. Invasive sensing and biochemical detection are beyond the scope of the present work and will be explored in future studies.

2. Literature Review

To achieve high-fidelity wearable physiological signal monitoring, the research community has conducted extensive exploration from multiple dimensions including materials, structures, actuation, and control. This section will review the current research status of flexible sensor material and structural design, active morphology control technology, lattice metamaterial applications, and photo-driven soft material systems, and on this basis, demonstrate the innovation and necessity of this study.

2.1. Material and Structural Design of Flexible Sensors

The core of flexible sensors lies in their ability to maintain stable electrical performance while conformally fitting with soft, irregular human body surfaces. This capability primarily depends on innovation at two levels: flexibilization of conductive materials and mechanical design of device structures. At the material level, extensive efforts have been devoted to developing materials that simultaneously exhibit

high conductivity and mechanical compliance. Conductive polymers, such as poly (3,4-ethylenedioxythiophene): poly(styrenesulfonate) (PEDOT:PSS), are widely adopted for constructing bioelectrodes due to their favorable biocompatibility and mixed ionic–electronic conduction characteristics [21]. However, their intrinsic brittleness limits performance under large deformation conditions.

To address this limitation, nanomaterial-based conductive networks, including silver nanowires, carbon nanotubes, and graphene, have been incorporated into polymer matrices to form percolated conductive pathways that can tolerate stretching through sliding and reconnection mechanisms [22, 23]. In parallel, mechanical structural design has been extensively explored to enhance device-level flexibility. Inspired by natural morphologies and origami/kirigami concepts, wavy, serpentine, and island–bridge architectures have been developed to redistribute strain and reduce stress concentration in functional regions [24, 25].

Despite these advances, such material and structural strategies remain fundamentally passive. Once fabricated, their morphology and mechanical response are fixed, preventing dynamic regulation of contact pressure or effective contact area in response to time-varying skin deformation, muscle contraction, or sweat-induced surface changes. As a result, contact degradation and signal instability remain unavoidable under realistic motion conditions.

2.2. Active Morphology Control Technology

To break through the limitations of passive adaptation, researchers have begun exploring ways to endow flexible devices with the ability to actively change their own shapes. Shape memory polymers (SMPs) and shape memory alloys (SMAs) are earlier studied actuation materials that can recover to preset shapes under specific stimuli (usually heat) [25]. However, their slow response speed (usually at tens of seconds to minutes level), poor cycling stability, and need for overall heating limit their development in wearable applications requiring rapid, local response. Electroactive polymers (EAPs) are another major class of actuation materials receiving attention, including ionic polymer-metal composites (IPMCs) and dielectric elastomer actuators (DEAs). IPMCs can be driven at low voltages but have small actuation force and need to work in humid environments. In contrast, DEAs can generate large strains and forces with fast response speed, but their actuation typically requires voltages up to kilovolts, bringing serious safety hazards and complex power management issues [11]. Magnetically responsive soft composites are made by embedding magnetic particles (such as NdFeB or Fe_3O_4) in elastomer matrices and can achieve non-contact wireless driving through external magnetic fields [12]. This method is safe with fast response, but magnetic field spatial resolution is limited, making it difficult to achieve fine local morphology control, and external magnet or electromagnetic coil systems are relatively bulky, unsuitable for integration into lightweight wearable devices.

Collectively, existing active actuation strategies face a trade-off between response speed, spatial controllability, safety, and system integration, leaving a critical gap for actuation mechanisms that can deliver localized, fast, and safe morphology regulation in wearable devices.

2.3. Applications of Lattice Metamaterials in Flexible Systems

Lattice metamaterials, as an emerging structural material, can exhibit extraordinary physical properties not possessed by natural materials macroscopically through rational design of their microscopic topological units' geometric configurations, such as negative Poisson's ratio, high strength-to-weight ratio, and programmable mechanical response [17, 26]. These properties show tremendous potential in flexible system design. Through additive manufacturing technologies such as 3D printing, lattice materials with complex three-dimensional network structures can be precisely manufactured [27]. In the soft robotics field, lattice structures are used to construct lightweight robot skeletons or achieve rapid shape switching through designing bistable units [28]. In the flexible electronics field, researchers utilize the porosity and compressibility of lattice structures to design pressure sensors. For example, Yin et al. used digital light processing (DLP) 3D printing technology to manufacture flexible pressure sensors with programmable lattice structures, achieving regulation of sensor sensitivity and measurement range by adjusting lattice geometric parameters [29]. However, current research mostly treats lattice structures as passive mechanical enhancement or sensing elements, with few studies exploring how to combine active driving mechanisms with lattice structures and utilize their unique structural advantages to achieve more efficient and complex morphology control.

2.4. Photo-Driven Soft Material Systems

Light, as an external stimulus source, has unique advantages such as wireless, sourceless, high spatiotemporal resolution, and no electromagnetic interference, making it an ideal choice for driving soft materials [13]. Photo-driving is usually divided into photochemical and photothermal mechanisms. Photochemical driving relies on reversible isomerization reactions of molecules under light irradiation (such as azobenzene), thereby causing macroscopic deformation of materials, but its response speed and driving force are usually small. In contrast, photothermal driving mechanisms are more common and efficient. This mechanism converts light energy into thermal energy efficiently by doping photothermal conversion agents (such as carbon nanotubes, graphene, gold nanorods, or conductive polymers) in materials, thereby triggering phase transitions or volume changes in temperature-sensitive matrix materials (such as PNIPAM hydrogel or liquid crystal elastomers), generating driving force [14, 30]. Particularly, PNIPAM hydrogel is in a hydrophilic swollen state below its lower critical solution temperature (LCST, ~32°C), and when temperature rises above LCST, it transforms into a hydrophobic contracted state, expelling internal water and producing rapid and significant volume changes [16]. Through high-precision processing technologies such as femtosecond laser direct writing, photo-responsive hydrogels with complex three-dimensional microstructures can be constructed, and through precise control of laser scanning paths, programming control of soft robot motion modes can be achieved [15]. This technology has been successfully used to drive various complex actions of micro-robots such as walking, swimming, grasping, and releasing, demonstrating its unparalleled control precision at microscopic scales.

3. METHODS

This study adopts a research strategy combining theoretical design, simulation modeling, and experimental verification to systematically develop and evaluate photo-driven lattice flexible sensor arrays. The methodological framework is designed to ensure structural reproducibility, controlled experimental conditions, and quantitative performance evaluation. This section elaborates on the structural design, material preparation, manufacturing process, photo-driven morphology control system, and experimental methods for performance characterization and data analysis of the sensor array.

3.1. Research Strategy

The overall technical route of this study follows the logical flow of "structural design → manufacturing characterization → deformation performance → sensing optimization → application verification". First, based on the design concept of mechanical metamaterials, we constructed truncated octahedral lattice structure models with different geometric parameters and preliminarily evaluated their mechanical and thermal characteristics through finite element analysis (FEA). The results were used to guide parameter selection rather than to replace experimental validation.

Next, high-precision laser direct writing (LDW) technology was employed to fabricate flexible sensor substrates with predefined lattice architectures using photo-responsive hydrogels, followed by the integration of conductive polymers to form sensing electrodes. Subsequently, an integrated laser scanning system combined with microscopic imaging was established to enable precise control and real-time observation of the photo-driven morphology control process. The effects of lattice geometry and laser parameters on deformation amplitude and response speed were systematically investigated under identical environmental conditions.

To verify sensing effectiveness, sensor arrays were attached to human skin and biomimetic skin models. Changes in contact impedance before and after active morphology control were quantitatively measured, while physiological signals including electrocardiogram (ECG) and electromyogram (EMG) were synchronously collected. Signal quality improvement was evaluated using metrics such as signal-to-noise ratio (SNR) and baseline drift. Finally, a closed-loop control algorithm was implemented to demonstrate adaptive fitting and stable monitoring under simulated dynamic conditions (e.g., joint bending). Throughout the study, control groups consisting of solid-structure sensors fabricated from identical materials were included to isolate the effect of lattice architecture.

3.2. Design of Lattice Sensor Array

To maximize flexibility and driving efficiency while maintaining structural integrity, the truncated octahedron was selected as the basic unit of the lattice network. This topology provides a balanced combination of isotropy, node connectivity, and porosity. Key geometric parameters include unit rod length (L) and rod diameter (D). By adjusting these parameters, the relative density (ρ_rel), defined as the ratio of lattice solid volume to the envelope volume, can be precisely controlled.

In this study, five lattice configurations with relative densities of 10%, 15%, 18.5%, 22%, and 25% were designed to systematically investigate their influence on mechanical properties and photo-driven deformation behavior. All lattice designs were generated using identical boundary dimensions to ensure comparability across samples. The overall sensor size was fixed at 8 × 8 × 2 mm³, comprising a 3 × 3 array of sensing units.

A PEDOT:PSS conductive layer with a thickness of approximately 500 nm was deposited on the top surface of each sensing unit via inkjet printing to serve as the sensing electrode. Electrodes were connected to external data acquisition systems using screen-printed silver paste leads. This integrated design enables the co-localization of actuation (hydrogel lattice) and sensing (PEDOT:PSS electrodes) within a unified flexible platform, minimizing mechanical mismatch.

3.3. Material Preparation and Manufacturing Process

Photo-responsive Hydrogel Precursor Preparation: The photo-responsive hydrogel precursor solution consists of N-isopropylacrylamide (NIPAM, 98%, Sigma-Aldrich) as the temperature-sensitive monomer, N, N′-methylenebisacrylamide (BIS, 99%, Sigma-Aldrich) as the chemical crosslinker, and 2-hydroxy-2-methyl-1-phenyl-1-propanone (Irgacure 1173, 97%, Sigma-Aldrich) as the photoinitiator. To impart photothermal responsiveness, single-walled carbon nanotubes (SWNTs, >95%, XFNANO) were uniformly dispersed in deionized water as photothermal conversion agents.Specifically, 780 mg of NIPAM, 15.6 mg of BIS, and 30 μL of Irgacure 1173 were dissolved in 5 mL of deionized water containing 0.1 mg/mL SWNTs. The mixture was ultrasonicated at room temperature for 30 min until a homogeneous and optically transparent precursor solution was obtained. All precursor solutions were freshly prepared prior to fabrication to minimize variability induced by aging effects.

Laser Direct Writing (LDW) Manufacturing: Lattice structures were fabricated using laser direct writing based on two-photon polymerization (TPP) (Nanoscribe Photonic Professional GT). The precursor solution was deposited onto plasma-treated glass substrates, and a 780 nm femtosecond laser was focused inside the solution through a 25× objective lens (NA = 0.8). A high-precision piezoelectric nano-positioning stage guided the laser focal point along predefined three-dimensional trajectories, inducing localized two-photon polymerization and enabling point-by-point, layer-by-layer construction of the lattice architecture. Laser power was set to 45 mW with a scanning speed of 100 μm/s. These parameters were kept constant for all samples unless otherwise specified. After fabrication, samples were sequentially rinsed in isopropanol and deionized water to remove unreacted monomers and photoinitiators, yielding free-standing hydrogel lattice structures.

Electrode Integration and Device Encapsulation: The cleaned hydrogel lattice samples were transferred onto flexible polyethylene terephthalate (PET) substrates. PEDOT:PSS aqueous dispersion (Clevios PH1000) was printed onto the top surface of each sensing unit using a micro inkjet printing system (Dimatix DMP-2831). Printed samples were dried at 60 °C for 15 min. External electrical connections were formed using conductive silver paste and flexible printed circuit boards (FPC). Finally, the entire device was encapsulated with a thin (~50 μm) layer of biocompatible silicone rubber (PDMS, Sylgard 184), leaving the electrode surfaces exposed. This encapsulation strategy enhances mechanical robustness while maintaining skin compatibility.

3.4. Photo-Driven Morphology Control System

A customized photo-driven morphology control system was developed to achieve precise actuation and synchronous observation of sensor deformation. The system consists of a continuously tunable 780 nm femtosecond laser (Coherent, Chameleon Vision II), a two-dimensional galvanometer scanning module (Thorlabs, GVS012), and an inverted optical microscope (Nikon, Eclipse Ti-U). The laser beam was guided through the galvanometer system and focused onto the sensor surface via the microscope objective.

Computer-controlled galvanometer deflection enabled programmable scanning paths, scanning speeds, and laser

power distributions. All actuation experiments were conducted under identical ambient conditions to minimize environmental interference. Real-time deformation processes were recorded using a CCD camera synchronized with the microscope. Three representative scanning strategies were designed to realize multimodal morphology control: (1) Linear scanning: Perform reciprocating linear scanning in the center area of sensing units to induce local contraction, forming "protrusion" mode; (2) Circular scanning: Perform circular path scanning along sensor array edges to produce non-uniform contraction, achieving overall "bending"; (3) Spiral scanning: Perform spiral path scanning from center outward or from outside to center to trigger torsional stress, achieving "torsion" deformation.

3.5. Data Collection Methods

Deformation Performance Measurement: Sensor deformation processes were recorded using a high-speed camera (Phantom VEO 710L) at 100 frames per second, synchronized with the photo-driven actuation system. Displacement, shrinkage ratio, and deformation speed were extracted using customized MATLAB-based image processing algorithms. Each deformation test was repeated at least three times to ensure measurement consistency.

Contact Impedance Measurement: Sensor arrays were attached to biomimetic skin models fabricated from conductive agarose gel. Contact impedance between sensor electrodes and the biomimetic skin was measured using a two-electrode configuration with an electrochemical workstation (CHI 660E) over a frequency range of 1 Hz to 100 kHz. Measurements were conducted prior to actuation and under different morphology control modes to evaluate the effect of active fitting on interfacial impedance.

Physiological Signal Collection: Healthy volunteers (n = 5, 25 ± 3 years old) were recruited for physiological signal acquisition. All experimental procedures involving human participants were approved by the relevant ethics committee, and informed consent was obtained from all participants prior to testing. Sensor arrays were placed at standard ECG lead positions (e.g., chest V4) and on the forearm extensor muscle group. ECG and EMG signals were synchronously recorded using a multi-channel physiological acquisition system (BIOPAC MP160). Tests were conducted under resting conditions and controlled motion states (e.g., arm bending and slow jogging) to compare signal quality before and after photo-driven morphology control.

3.6. Data Analysis Methods

Finite Element Simulation: Physiological signals were digitally filtered (ECG: 0.5–100 Hz bandpass; EMG: 20–500 Hz bandpass). Signal-to-noise ratio (SNR) was calculated as the ratio of dominant signal peak energy to baseline noise energy, while baseline wander was quantified using the standard deviation of the signal baseline. Motion artifacts were evaluated by comparing signal energy differences between motion and resting states. All quantitative data are presented as mean ± standard deviation. Statistical significance was assessed using two-tailed Student's t-tests, with $p < 0.05$ considered statistically significant.

Signal Quality Evaluation: Physiological signals were digitally filtered (ECG: 0.5–100 Hz bandpass; EMG: 20–500 Hz bandpass). Signal-to-noise ratio (SNR) was calculated as the ratio of dominant signal peak energy to baseline noise energy, while baseline wander was quantified using the standard deviation of the signal baseline. Motion artifacts were evaluated by comparing signal energy differences between motion and resting states. All quantitative data are presented as mean ± standard deviation. Statistical significance was assessed using two-tailed Student's t-tests, with $p < 0.05$ considered statistically significant.

4. DATA

All experiments in this study were conducted under strictly controlled conditions to ensure data reliability and reproducibility. This section focuses on the composition and consistency of experimental samples, the descriptive statistical characteristics of key structural and performance variables, and the standardized data preprocessing procedures applied prior to quantitative analysis.

4.1. Experimental Sample Information

According to the design scheme described in Section 3.2, a total of six types of sensor array samples were fabricated. Five types correspond to lattice-structured sensors with relative densities of 10%, 15%, 18.5%, 22%, and 25%, respectively, while one type consists of a solid-structure sensor (relative density of 100%) serving as the control group. For each sensor type, three independent replicate samples were prepared, resulting in a total of 18 sensor arrays for subsequent performance evaluation.

All samples were fabricated using the same batch of hydrogel precursor solution and processed under identical laser direct writing and post-fabrication conditions to minimize batch-to-batch variability. Performance testing was conducted in a standard laboratory environment with temperature maintained at 25 ± 2 °C and relative humidity at 50 ± 10%. These environmental parameters were kept constant throughout all measurements to ensure data comparability across different sample groups.

Biomimetic skin models used for contact impedance and physiological signal testing were prepared from 2% agarose gel containing 0.9% sodium chloride solution, which provides electrical conductivity comparable to that of human skin and enables repeatable interfacial measurements under controlled conditions.

4.2. Descriptive Statistics of Key Variables

Manufactured lattice structures were characterized using scanning electron microscopy (SEM) and optical profilometry to obtain precise geometric measurements. The descriptive statistical results of key structural, deformation, and electrical performance parameters are summarized in Table 1. Across all lattice samples, manufacturing deviations in rod length (L) and rod diameter (D) were controlled within ±5%, indicating high fabrication fidelity and structural consistency.

During photo-driven deformation testing, the lattice structure with a relative density of 18.5% exhibited the most balanced overall performance. The mean maximum linear shrinkage rate reached 35.2%, with a standard deviation of 2.8%, while the average deformation speed was 12.8 μm/s with a standard deviation of 1.5 μm/s. These values reflect stable actuation behavior across independent samples rather than isolated peak performance.

In terms of electrical performance, the mean contact impedance of sensors in the initial fitting state was 18.5 kΩ (standard deviation: 3.2 kΩ). After photo-driven morphology optimization, the contact impedance decreased to a mean

value of 7.0 kΩ with a standard deviation of 1.5 kΩ. The reduction in impedance demonstrates improved interfacial contact quality following active morphology control.

TABLE I. DESCRIPTIVE STATISTICS OF KEY VARIABLES

Parameter Category	Variable Name	Mean	Std Dev	Unit
Structural Parameters	Rod Length (L)	6.2	0.3	μm
	Rod Diameter (D)	5.1	0.2	μm
	Array Size	8×8×2	-	mm³
Deformation Performance	Max Shrinkage (ρ_rel=18.5%)	35.2	2.8	%
(Optimal Sample)	Deformation Speed (ρ_rel=18.5%)	12.8	1.5	μm/s
Electrical Performance	Initial Contact Impedance	18.5	3.2	kΩ
	Optimized Contact Impedance	7.0	1.5	kΩ

4.3. Data Preprocessing Methods

To ensure analysis accuracy, all raw data underwent standardized preprocessing procedures. Deformation process videos recorded using high-speed cameras were processed through MATLAB's image processing toolbox, including Gaussian filtering for denoising, binarization to segment targets from backgrounds, and centroid tracking algorithms to extract displacement-time data. Impedance spectrum data exported from electrochemical workstations were fitted using Z-View software for equivalent circuit fitting to separate contact resistance and capacitance components. Raw physiological signal data collected from BIOPAC systems were imported into AcqKnowledge software for processing. ECG signals passed through a 0.5-100 Hz bandpass filter to eliminate baseline drift and high-frequency noise; EMG signals passed through a 20-500 Hz bandpass filter. All filtered data underwent baseline correction and normalization processing to eliminate individual differences and DC offset effects, facilitating subsequent SNR calculation and statistical comparative analysis.

5. RESULTS

This section systematically presents the experimental results of the photo-driven lattice flexible sensor arrays, including their fabrication quality and structural characterization, photo-driven deformation performance, multi-modal morphology control capability, and application performance in contact impedance optimization and physiological signal quality enhancement. The results are presented with an emphasis on quantitative comparison and mechanism-oriented interpretation.

5.1. Manufacturing and Characterization of Lattice Sensor Arrays

Flexible sensor arrays with well-defined three-dimensional truncated octahedral lattice architectures were successfully fabricated using laser direct writing technology. Figure 1A illustrates the complete fabrication workflow, including structural design, laser direct writing, and electrode integration. Scanning electron microscopy (SEM) images reveal the microscopic morphology of lattice structures with different relative densities (Figure 1B), demonstrating highly uniform, periodic networks with no observable structural collapse or defects.

X-ray micro-computed tomography (Micro-CT) three-dimensional reconstructions further confirm the high consistency between the fabricated lattice structures and the corresponding design models (Figure 1C). These results indicate that the LDW process enables accurate reproduction of complex three-dimensional lattice geometries across different density levels. Mechanical testing shows that the effective Young's modulus of the lattice structures increases monotonically with relative density. However, within the tested density range (10%–25%), the modulus values (0.5–2.1 MPa) remain substantially lower than that of the solid hydrogel structure (12.4 MPa), highlighting the pronounced flexibility advantage introduced by lattice architecture (Figure 1D).

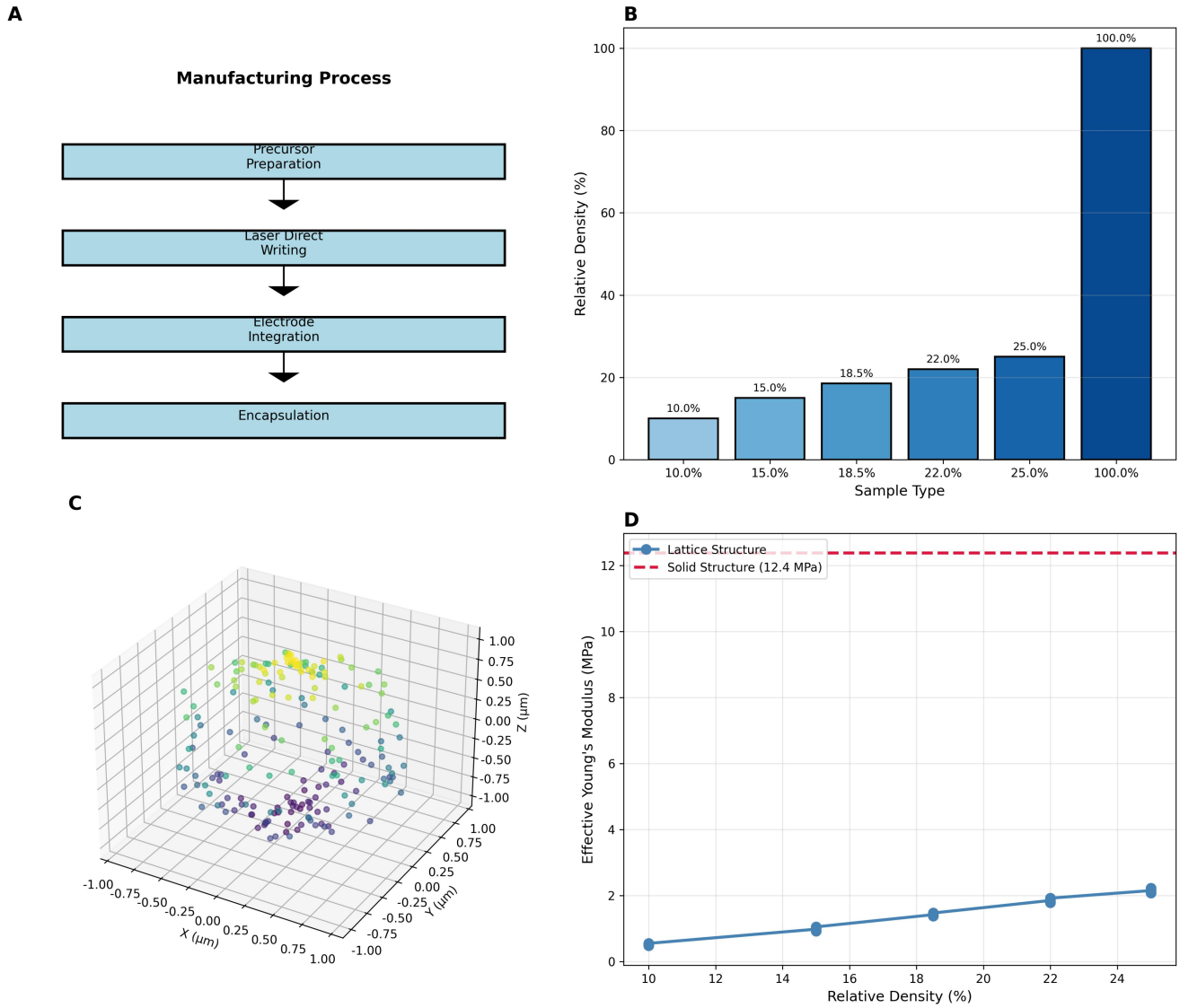

Figure 1. Design, Manufacturing and Characterization of Lattice Sensor Arrays

5.2. Photo-Driven Deformation Performance

The introduction of lattice architecture significantly enhances the photo-driven deformation performance of the sensor arrays. Under identical laser irradiation conditions (60 mW), the lattice structure with a relative density of 18.5% exhibits a maximum linear shrinkage rate of 35.2%, which is approximately 3.2 times higher than that of the solid structure fabricated from the same material (shrinkage rate of 11.0%) (Figure 2A and 2B). Similarly, the average deformation speed of the lattice structure reaches 12.8 μm/s, representing a 3.7-fold increase compared with the solid counterpart (3.5 μm/s) (Figure 2C).

This performance enhancement can be attributed to the porous lattice configuration, which reduces global mechanical constraints and facilitates localized contraction. In addition, the increased specific surface area promotes photothermal conversion efficiency, while the interconnected pore network shortens water diffusion pathways, thereby accelerating thermal response and mass transfer processes. These mechanisms are further supported by the optical–thermal–mechanical coupled finite element simulations. As shown in Figure 2D, lattice structures exhibit faster temperature rise and more favorable stress distributions for macroscopic deformation under identical irradiation conditions.

The influence of laser power and scanning frequency on deformation behavior was also investigated. Both deformation amplitude and deformation speed increase with laser power and show a positive correlation with scanning frequency within a defined operational range (Figure 2E and 2F). These results provide quantitative guidance for subsequent morphology programming and adaptive control.

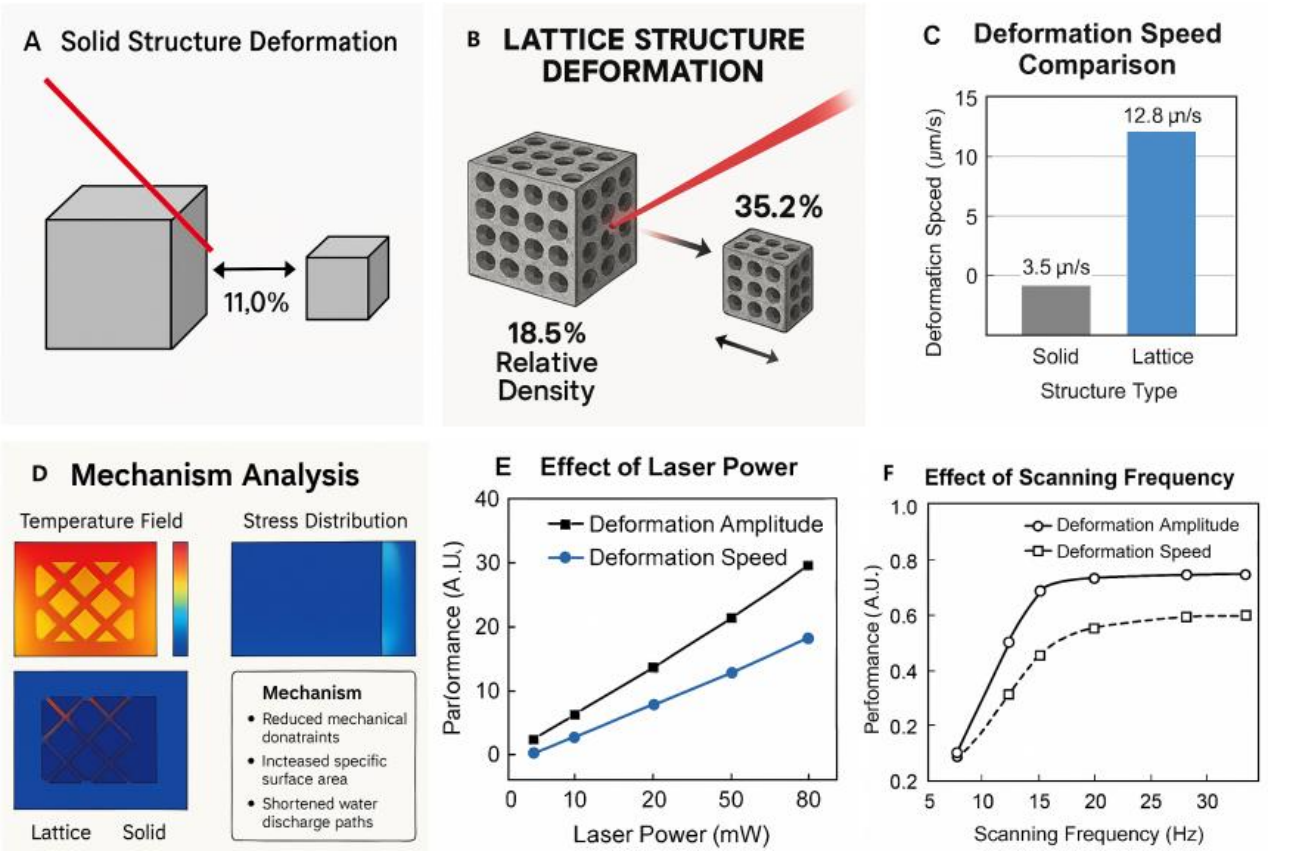

Figure 2. Photo-Driven Deformation Performance Analysis and Comparison

5.3. Multi-Modal Morphology Control

By programming laser scanning trajectories, three distinct and controllable morphology modes were achieved (Figure 3). Linear scanning at the center of a single sensing unit induces localized hydrogel contraction, resulting in an upward protrusion of the electrode surface. This "local protrusion" mode reaches a maximum protrusion height of approximately 180 µm (Figure 3A), enabling active enhancement of contact pressure in recessed skin regions.

Circular scanning along the periphery of the sensor array produces non-uniform edge contraction, leading to an overall bending deformation with a minimum curvature radius of 6 mm (Figure 3B). This bending mode allows the sensor array to conform closely to curved anatomical surfaces such as wrists and forearms. Spiral scanning paths generate torsional stress through spatially non-uniform contraction, resulting in a torsion mode with a maximum torsion angle of 18° (Figure 3C).

All three deformation modes exhibit good reversibility and repeatability, with response times within 5 s. The availability of multiple deformation modes enables the sensor arrays to actively adapt to complex surface geometries and dynamic morphological changes of the human body.

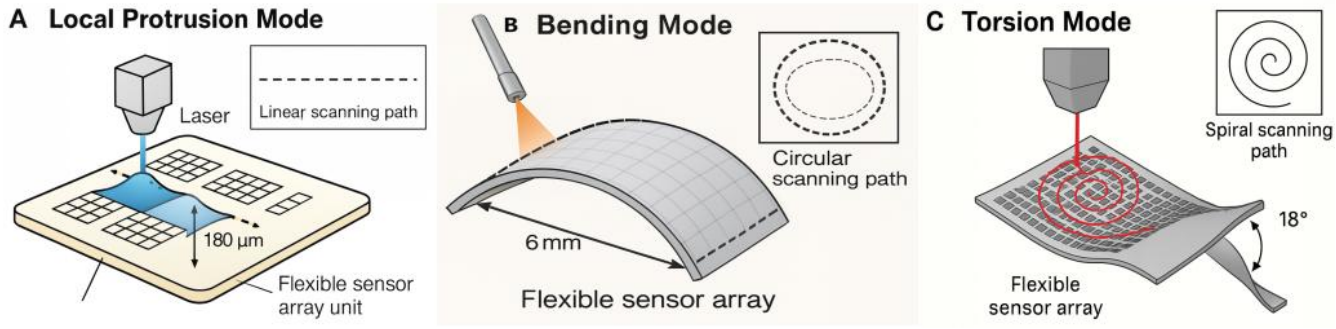

Figure 3. Implementation and Characterization of Multi-Modal Morphology Control

5.4. Contact Impedance Optimization

Active morphology control leads to a pronounced reduction in contact impedance at the sensor–skin interface. When attached to biomimetic skin models, sensors without photo-driven control exhibit an initial contact impedance of 18.5 ± 3.2 kΩ at 1 kHz. Activation of the "local protrusion" mode rapidly decreases the contact impedance to 7.0 ± 1.5 kΩ, corresponding to a reduction of 62.3% (Figure 4A and 4B).

Under simulated joint bending conditions, sensors without active control experience severe impedance increases exceeding 50 kΩ due to partial detachment. In contrast, when the "bending" mode is activated to accommodate substrate deformation, the contact impedance is stably maintained below 10 kΩ (Figure 4C). These results demonstrate that active morphology control effectively mitigates contact instability induced by dynamic mechanical deformation.

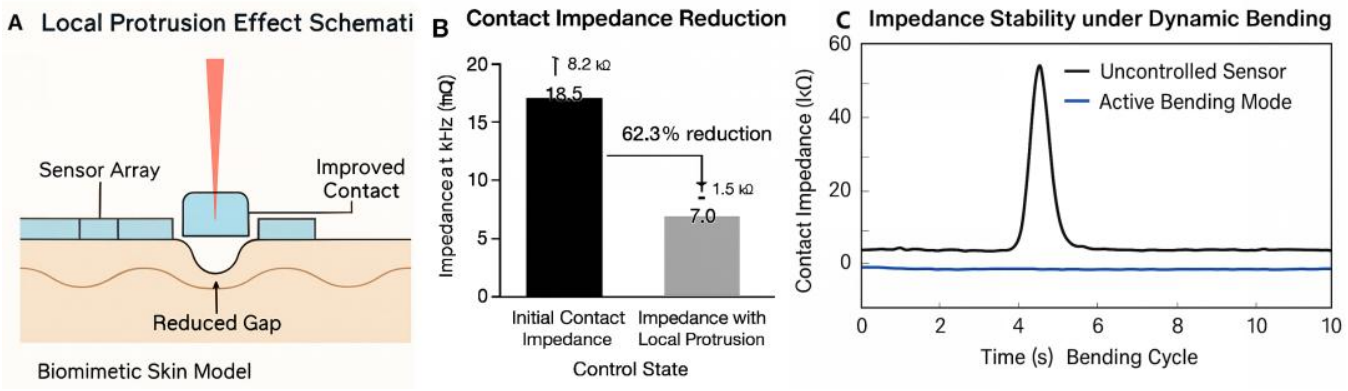

Figure 4. Optimization Effect of Active Morphology Control on Contact Impedance

5.5. *Physiological Signal Quality Improvement*

Effective reduction of contact impedance directly translates into significant improvement of physiological signal quality. In ECG signal monitoring experiments, when volunteers were in resting state, activating morphology control improved signal-to-noise ratio (SNR) from 32.5 dB to 47.7 dB. In simulated motion (arm swinging) states, optimization effects were more significant: without control, signals were strongly submerged by motion artifacts with SNR dropping to 15.1 dB; while after activating active control, sensors could effectively compensate for contact instability caused by motion, with SNR recovering to 33.8 dB, improving by 18.7 dB, and ECG waveform P-QRS-T features becoming clearly distinguishable (Figure 5A, 5B). In EMG signal monitoring, morphology control increased signal amplitude by an average of 2.1 times, and in continuous hand action recognition tasks, classification accuracy based on controlled signals improved from 78% without control to 95% (Figure 5C). For body temperature monitoring, active fitting eliminated air gaps between sensor and skin, reducing temperature measurement response time from 12.5 seconds to 4.2 seconds with accuracy reaching ±0.15°C.

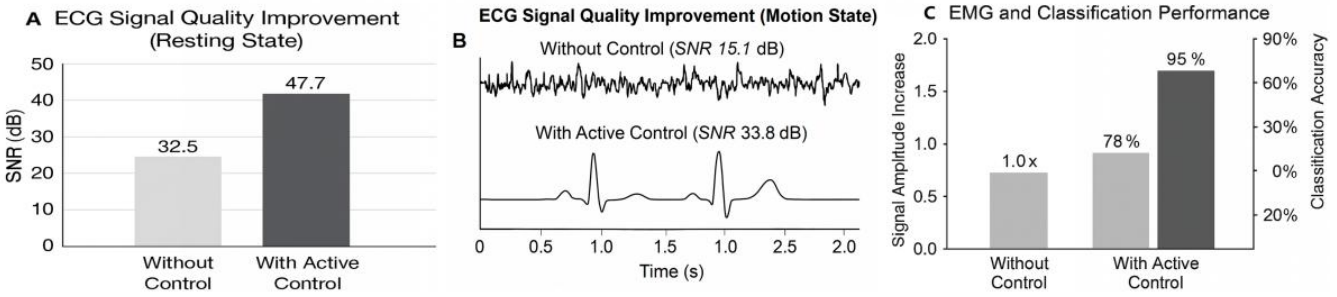

Figure 5. Improvement Effect of Active Morphology Control on Physiological Signal Quality

5.6. *Closed-Loop Adaptive Control*

To further enhance sensor intelligence, a closed-loop adaptive control system based on real-time signal quality feedback was developed. The system continuously evaluates signal-to-noise ratio and baseline drift. When signal quality falls below predefined thresholds, the controller automatically adjusts laser scanning parameters, including irradiation position and power, to locally modify sensor morphology until signal quality is restored.

Figure 6 illustrates the closed-loop control performance during continuous elbow flexion and extension. When joint motion induces signal degradation at the sensor edges, the system autonomously triggers a combination of "bending" and "protrusion" modes to re-establish stable contact. As a result, the ECG signal SNR is maintained consistently above 30 dB throughout the motion cycle. The adaptive adjustment process is completed within approximately 10 s, demonstrating the feasibility of autonomous, real-time contact optimization under dynamic conditions.

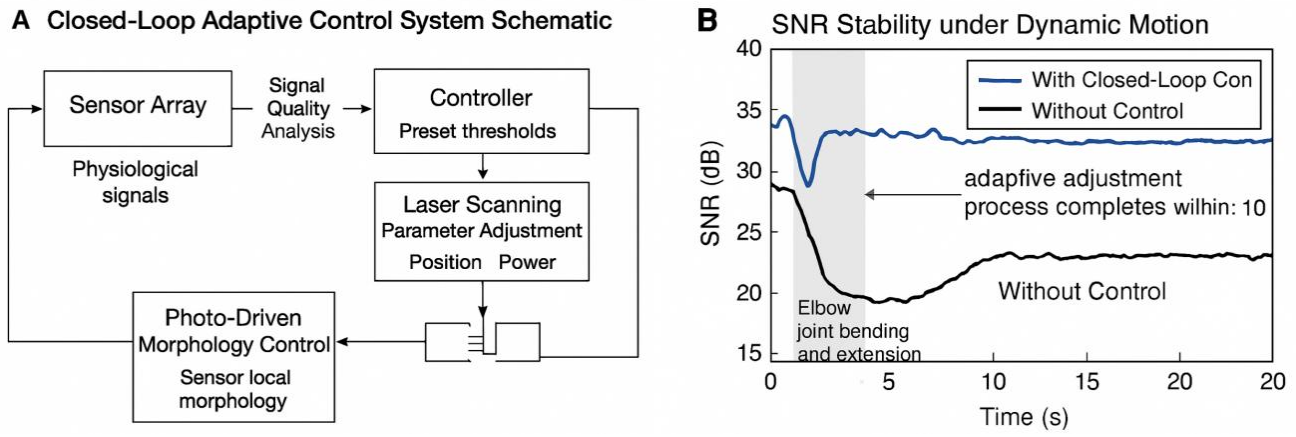

Figure 6. Demonstration of Closed-Loop Adaptive Control System

6. Discussion

This study integrates photo-driven soft materials, lattice metamaterial design, and flexible sensing technology to develop an intelligent sensor array capable of actively modulating its morphology to optimize signal acquisition quality. The experimental results demonstrate the feasibility and effectiveness of this integrated strategy in addressing dynamic contact instability in wearable sensing. Rather than introducing a single material or device innovation, this work provides a system-level solution that links structural design, actuation mechanism, and sensing performance. In this section, the underlying physical mechanisms, technical advantages, design implications, and inherent limitations are discussed in a balanced and objective manner.

6.1. Enhancement Mechanism of Lattice Structure on Driving Performance

A central contribution of this work lies in the use of lattice metamaterial architectures to substantially enhance the photo-driven actuation performance of hydrogels. Experimental results show that, compared with solid structures, the lattice configuration with a relative density of 18.5% achieves more than a threefold increase in both shrinkage amplitude and response speed. This enhancement arises from the synergistic coupling of mechanical deformation modes and thermodynamic transport processes enabled by the lattice geometry.

From a mechanical perspective, the porous lattice network significantly reduces macroscopic constraints. In solid hydrogels, photothermally induced local contraction is strongly restricted by surrounding regions, resulting in energy dissipation through internal stress accumulation with limited global deformation. In contrast, lattice structures composed of slender rod-like elements primarily deform through rotation and bending rather than volumetric compression. Such rotation-dominated deformation represents a mechanically efficient pathway, allowing microscale contraction to be effectively translated into macroscale shape change.

From a thermodynamic and mass transfer perspective, lattice architectures increase the specific surface area and introduce interconnected microchannels throughout the material. This configuration enhances light absorption and heat transfer by photothermal agents (SWNTs) and, more importantly, facilitates rapid water expulsion during hydrogel phase transition. Unlike solid hydrogels, where water transport relies on slow diffusion, lattice structures enable direct and distributed fluid release through open pores, substantially shortening the response time. Finite element simulations further support this interpretation, revealing faster temperature rise and stress localization at lattice nodes, which promotes rod rotation and global deformation, in good agreement with experimental observations.

6.2. Technical Advantages and Design Connotations of Active Morphology Control

Compared with conventional passive flexible sensors and other active actuation strategies, the photo-driven approach presented here exhibits several distinct technical advantages. Passive structural designs, such as serpentine or island–bridge layouts, improve mechanical compliance but remain intrinsically static. They lack the ability to actively and locally respond to dynamic changes at the sensor–skin interface caused by motion, sweating, or muscle contraction.

In contrast, the proposed sensor array enables dynamic, spatially selective, and programmable contact optimization through controlled laser scanning. Specific deformation modes—protrusion, bending, and torsion—can be generated at predefined locations to address different contact challenges. For example, the “local protrusion” mode compensates for insufficient contact pressure caused by skin depressions or partial detachment, a function that passive sensors cannot achieve.

Relative to other active actuation technologies, photo-driven control avoids the high driving voltages required by dielectric elastomer actuators and does not depend on bulky external magnetic components. The use of femtosecond laser scanning enables micrometer-scale spatial resolution, exceeding that of magnetic or global thermal actuation methods. From a design perspective, this work illustrates a design-driven integration strategy: rather than optimizing materials or devices in isolation, the system is constructed around a clearly defined application challenge—dynamic contact failure—by combining metamaterial mechanics, optical actuation, and soft sensing into a unified framework. This approach highlights how structural design can serve as a functional mediator between actuation physics and sensing performance.

6.3. Significance of Improving Physiological Signal Quality

The experimental results demonstrate that active morphology control leads to substantial improvements in

physiological signal quality. Under motion conditions, ECG signal-to-noise ratio increases by 18.7 dB, representing a level of enhancement with clear practical significance. In signal processing terms, a 3 dB increase corresponds to a halving of noise power; therefore, an 18.7 dB improvement indicates a drastic suppression of motion-induced artifacts. This level of noise reduction enables reliable extraction of key ECG features, such as P–QRS–T complexes, even during dynamic activity.

Similar benefits are observed in EMG monitoring, where increased signal amplitude and improved classification accuracy enhance the reliability of muscle activity recognition. These results suggest that improving wearable signal quality should not rely exclusively on post hoc algorithmic filtering, but should instead address the physical origin of signal degradation at the sensor–skin interface. By actively stabilizing and optimizing contact conditions, the proposed strategy reduces artifact generation at its source, providing a complementary pathway to conventional signal processing approaches.

6.4. Limitations and Future Prospects

Despite the promising results, several limitations must be addressed before practical deployment. First, system portability remains a major challenge. The current implementation relies on a femtosecond laser and galvanometer scanning system, which is not suitable for daily wearable use. Future efforts should focus on replacing bulk optical systems with compact and integrated light sources, such as fiber-coupled micro-lasers or addressable micro-LED arrays embedded within flexible substrates.

Second, long-term biocompatibility and stability require further investigation. Although PDMS encapsulation improves robustness, material degradation, electrode stability, and potential thermal effects on skin under prolonged wear—particularly in the presence of sweat and friction—must be evaluated through extended in vivo studies. Third, while the response speed is significantly improved, second-scale actuation may still be insufficient for capturing extremely fast physiological events, such as neural signals. Further advances in hydrogel chemistry and lattice topology optimization are needed to accelerate phase transition kinetics and mass transport.

Finally, manufacturing scalability represents a practical bottleneck. Laser direct writing offers high precision but suffers from low throughput and high cost. Exploring scalable fabrication techniques, including projection lithography, soft molding, or extrusion-based additive manufacturing, will be critical for translating this technology toward large-scale production. In future work, integrating closed-loop control with machine learning algorithms may enable predictive morphology adjustment based on individual motion patterns, paving the way for more personalized and intelligent wearable sensing systems.

7. Conclusion

This study addresses the core challenge of signal quality degradation caused by poor contact in flexible wearable sensors in dynamic physiological environments by proposing and implementing an adaptive flexible sensor array based on photo-driven lattice metamaterials. By combining photo-responsive hydrogel with carefully designed truncated octahedral lattice structures, we successfully manufactured an intelligent sensing platform capable of achieving multi-modal, large-range, rapid morphology control through laser precise control. Research results show that lattice structure design improved photo-driven deformation capability by more than 3 times, and through active deformation modes such as "local protrusion", "bending", and "torsion", reduced contact impedance between sensor and skin by 62.3%, ultimately improving ECG signal-to-noise ratio by 18.7 dB under motion states. We further developed and verified a closed-loop adaptive control system, demonstrating the sensor's potential for autonomously maintaining high-quality monitoring in dynamic scenarios. This work introduces high-precision control strategies of photo-driven soft robots into wearable sensing fields for the first time, providing a paradigm shift from "passive adaptation" to "active control" for solving motion artifact problems. It not only provides a practical technical path for developing next-generation intelligent wearable health monitoring devices but also fully demonstrates the tremendous value of design-driven interdisciplinary research in catalyzing disruptive technologies. Future work will focus on miniaturization of driving systems, long-term biocompatibility assessment, and manufacturing process scalability to push this technology toward practical applications.

References

[1] Yuan, Y., et al. (2022). Flexible Wearable Sensors in Medical Monitoring. PMC. https://doi.org/10.3390/bios12121069

[2] Ha, M., Lim, S., & Ko, H. (2018). Wearable and flexible sensors for user-interactive health-monitoring devices. Journal of Materials Chemistry B, 6(24), 4043-4064. https://doi.org/10.1039/C8TB01063C

[3] Chen, S., et al. (2021). Flexible wearable sensors for cardiovascular health monitoring. Advanced Healthcare Materials. Https://doi.org/10.1002/adhm.202100116

[4] Ali, S. M., Noghanian, S., Khan, Z. U., Alzahrani, S., Alharbi, S., Alhartomi, M., & Alsulami, R. (2025). Wearable and flexible sensor devices: Recent advances in designs, fabrication methods, and applications. Sensors, 25(5), 1377. https://doi.org/10.3390/s25051377

[5] Vaghasiya, J. V., Mayorga-Martinez, C. C., & Pumera, M. (2023). Wearable sensors for telehealth based on emerging materials and nanoarchitectonics. npj Flexible Electronics, 7(1), 26. https://doi.org/10.1038/s41528-023-00261-4

[6] Wang, X., Liu, Z., & Zhang, T. (2017). Flexible sensing electronics for wearable/attachable health monitoring. Small, 13(25), 1602790. https://doi.org/10.1002/smll.201602790

[7] Ferreira, R. G., Silva, A. P., & Nunes-Pereira, J. (2024). Current on-skin flexible sensors, materials, manufacturing approaches, and study trends for health monitoring: a review. ACS sensors, 9(3), 1104-1133.

[8] Su, B., Li, J., Xu, H., Xu, Z., Meng, J., & Chen, X. (2022). Scientific training assistance: flexible wearable sensor motion monitoring applications. Chin. Sci. Inf. Sci, 52(1), 54-74.

[9] El-Atab, N., Mishra, R. B., Al-Modaf, F., Joharji, L., Alsharif, A. A., Alamoudi, H., ... & Hussain, M. M. (2020). Soft actuators for soft robotic applications: A review. Advanced Intelligent Systems, 2(10), 2000128. https://doi.org/10.1002/aisy.202000128

[10] Yasa, O., Toshimitsu, Y., Michelis, M. Y., Jones, L. S., Filippi, M., Buchner, T., & Katzschmann, R. K. (2023). An overview of soft robotics. Annual Review of Control, Robotics, and Autonomous Systems, 6(1), 1-29. https://doi.org/10.1146/annurev-control-062322-100607

[11] Xavier, M. S., Tawk, C. D., Fleming, A., Zolfagharian, A., Pinskier, J., Howard, D., ... & Bodaghi, M. (2022). Soft pneumatic actuators: A review of design, fabrication, modeling, sensing, control and applications. https://doi.org/10.1109/ACCESS.2022.3179589

[12] Teng, X., Gao, Z., Feng, X., Zhu, S., & Yang, W. (2025). Photothermal and Magnetic Actuation of Multimodal PNIPAM Hydrogel-Based Soft Robots. Gels, 11(9), 692. https://doi.org/10.3390/gels11090692

[13] Gao, Y., Wang, X., & Chen, Y. (2024). Light-driven soft microrobots based on hydrogels and LCEs: development and prospects. RSC advances, 14(20), 14278-14288. https://doi.org/10.1039/D4RA00495G

[14] Jiang, J., Xu, S., Ma, H., Li, C., & Huang, Z. (2023). Photoresponsive hydrogel-based soft robot: A review. Materials Today Bio, 20, 100657. https://doi.org/10.1016/j.mtbio.2023.100657

[15] Yu, H., Ding, H., Zhang, Q., Gu, Z., & Gu, M. (2021). Three-dimensional direct laser writing of PEGda hydrogel microstructures with low threshold power using a green laser beam. Light: Advanced Manufacturing, 2(1), 31-38. https://doi.org/10.37188/lam.2021.003

[16] Li, S., Cai, Z., Han, J., Ma, Y., Tong, Z., Wang, M., ... & Chen, X. (2023). Fast-response photothermal bilayer actuator based on poly (N-isopropylacrylamide)–graphene oxide–hydroxyethyl methacrylate/polydimethylsiloxane. RSC advances, 13(26), 18090-18098. https://doi.org/10.1039/D3RA03213B

[17] Jiao, P., Mueller, J., Raney, J. R., Zheng, X., & Alavi, A. H. (2023). Mechanical metamaterials and beyond. Nature communications, 14(1), 6004. https://doi.org/10.1038/s41467-023-41679-8

[18] Shojaee, M., Valizadeh, I., Klein, D. K., Sharifi, P., & Weeger, O. (2024). Multiscale modeling of functionally graded shell lattice metamaterials for additive manufacturing. Engineering with Computers, 40(3), 2019-2036. https://doi.org/10.1007/s00366-023-01906-8

[19] Beloshenko, V., Beygelzimer, Y., Chishko, V., Savchenko, B., Sova, N., Verbylo, D., ... & Vozniak, I. (2021). Mechanical properties of flexible tpu-based 3d printed lattice structures: Role of lattice cut direction and architecture. Polymers, 13(17), 2986. https://doi.org/10.3390/polym13172986

[20] Rivnay, J., Owens, R. M., & Malliaras, G. G. (2014). The rise of organic bioelectronics. Chemistry of Materials, 26(1), 679–685. https://doi.org/10.1021/cm4022003

[21] Amjadi, M., Kyung, K. U., Park, I., & Sitti, M. (2016). Stretchable, skin-mountable, and wearable strain sensors and their potential applications. Advanced Functional Materials, 26(11), 1678–1698. https://doi.org/10.1002/adfm.201504755

[22] Boland, C. S., Khan, U., Backes, C., O'Neill, A., McCauley, J., Duane, S., Shanker, R., Liu, Y., Jurewicz, I., Dalton, A. B., & Coleman, J. N. (2014). Sensitive, high-strain, high-rate bodily motion sensors based on graphene–rubber composites. ACS Nano, 8(9), 8819–8830. https://doi.org/10.1021/nn503454h

[23] Rogers, J. A., Someya, T., & Huang, Y. (2010). Materials and mechanics for stretchable electronics. Science, 327(5973), 1603–1607. https://doi.org/10.1126/science.1182383

[24] Xu, S., Zhang, Y., Jia, L., Mathewson, K. E., Jang, K. I., Kim, J., Fu, H., Huang, X., Chava, P., Wang, R., Bhole, S., Wang, L., Na, Y. J., Guan, Y., Flavin, M., Han, Z., Huang, Y., & Rogers, J. A. (2014). Soft microfluidic assemblies of sensors, circuits, and radios for the skin. Science, 344(6179), 70–74. https://doi.org/10.1126/science.1250169

[25] Lendlein, A., & Kelch, S. (2002). Shape-memory polymers. Angewandte Chemie International Edition, 41(12), 2034–2057. https://doi.org/10.1002/1521-3773(20020617)41:12<2034::AID-ANIE2034>3.0.CO;2-O

[26] Bertoldi, K., Vitelli, V., Christensen, J., & van Hecke, M. (2017). Flexible mechanical metamaterials. Nature Reviews Materials, 2, 17066. https://doi.org/10.1038/natrevmats.2017.66

[27] Zheng, X., Lee, H., Weisgraber, T. H., Shusteff, M., DeOtte, J., Duoss, E. B., Kuntz, J. D., Biener, M. M., Ge, Q., Jackson, J. A., Kucheyev, S. O., Fang, N. X., & Spadaccini, C. M. (2014). Ultralight, ultrastiff mechanical metamaterials. Science, 344(6190), 1373–1377. https://doi.org/10.1126/science.1252291

[28] Overvelde, J. T. B., Weaver, J. C., Hoberman, C., & Bertoldi, K. (2016). A three-dimensional actuated origami-inspired transformable metamaterial with multiple degrees of freedom. Nature Communications, 7, 10929. https://doi.org/10.1038/ncomms10929

[29] Yin, R., Wang, D., Zhao, S., Lou, Z., Shen, G., & Zhou, X. (2020). Programmable porous elastomeric lattice structures for flexible pressure sensors fabricated by digital light processing. Advanced Functional Materials, 30(6), 1908467. https://doi.org/10.1002/adfm.201908467

[30] Zhao, Q., Qi, H. J., & Xie, T. (2015). Recent progress in shape memory polymer: New behavior, enabling materials, and mechanistic understanding. Progress in Polymer Science, 49–50, 79–120. https://doi.org/10.1016/j.progpolymsci.2015.04.001

ACKNOWLEDGEMENTS

None.

FUNDING

None.

AVAILABILITY OF DATA

Not applicable.

ETHICAL STATEMENT

All participants provided written informed consent prior to participation. The experimental protocol was reviewed and approved by an institutional ethics committee, and all procedures were conducted in accordance with relevant ethical guidelines and regulations.

AUTHOR CONTRIBUTIONS

Reginald Makoa conceived the research concept, designed the photo-driven lattice sensor architecture, and led the experimental investigation and data analysis, while Fangtian Ying supervised the study, guided the interdisciplinary integration of design, materials, and sensing strategies, and critically revised the manuscript.

COMPETING INTERESTS

The authors declare no competing interests.